Inspection of Quince Slice Dehydration Stages based on Extractable Image Features

Abdolabbas JAFARI and Adel BAKHSHIPOUR

[1]*Farm Machinery Department, Shiraz University, Shiraz, Iran*

Abstract

Jafari A., Bakhshipour A. (2014): **Inspection of quince slice dehydration stages based on extractable image features.** Czech J. Food Sci., **32**: 456–463.

The relation between the moisture content of the fruit and image-based characteristics was investigated. Quince samples were dried in an oven dryer at three different temperatures (40, 50, and 60°C). Several shape, texture, and colour features of the quince slices were extracted from the images. Gradual reduction was observed in all morphological features when the moisture content of the samples decreased. Regression equations between the extracted features and moisture content of the quince slices were investigated. The moisture content prediction equations based on morphological features were more precise than the textural features while colour information did not yield any satisfactory result. To exploit the morphological and textural features simultaneously, several artificial neural network models were developed to predict the drying behaviour of quince. R^2 and RMSE values were determined as 0.998, 0.008%. It was concluded that the combination of the neural networks and image processing technique has the potential to determine the moisture variations.

Keywords: machine vision; neural networks; moisture content; drying; quince

During the drying processes, high moisture materials like fruits are exposed to physical and chemical changes. The quality of the dehydrated products is a complex result of the properties that characterise the final products, of which the most important one is colour (Kiranoudis & Markatos 2000). Researchers have been interested in the application of machine vision systems in various bioprocessing fields (Smékal *et al*. 2005; Firatligil-Durmus *et al*. 2008; Randulová *et al*. 2011; Golpour *et al*. 2014). Several features can be extracted from the images to be correlated with the quality of food products. Kit *et al*. (2004) presented a simple digital imaging method to measure and analyse the surface colour of food products. Morphological features are widely used in automated grading, sorting, and detection of objects in the industry (Jayas *et al*. 2000).

Shrinkage occurs during the fruits and vegetables dehydration when the viscoelastic matrix contracts into the space that was previously occupied by the water removed from the cells (Yadollahinia & Jahangiri 2009). Yadollahinia and Jahangiri (2009) used a method based on computer vision to analyse the effect of drying on potato slices shrinkage.

Image texture is an important image feature and has been applied greatly in the food industry (Wu *et al*. 2008). Fernández *et al*. (2005) investigated the effect of drying on shrinkage, colour, and some image texture features of apple discs. However, none of the above researches reported the suitable equations to estimate the moisture content (MC) during drying.

Machine vision has the potential to be used as a precise method for the recognition and assessment of apparent characteristics. It can be used to determine the qualitative characteristics of the product, provided that a strong correlation exists between the qualitative specifications and visual features. Therefore, in the presence of such relations, machine vision systems can be used in a dryer system to control the product quality in real time mode.

Artificial Neural Network (ANN) is one of the artificial intelligences widely used in the recent decade to simulate and predict useful parameters in drying. ANNs overcome the limitations of conventional ap-

proaches by extracting the desired information using the input data. It does not need specific equation forms. Instead, it needs sufficient input and output data (Menlik *et al*. 2010). Farkas *et al*. (2000) studied the application of ANNs in an agricultural fixed bed drier and concluded that the ANN could be effective for modelling the grain-drying process. Cubillos and Reyes (2003) also designed an ANN to model the drying of carrots. Based on these useful characteristics of machine vision and neural network, it seems that a real time inspection system can be utilised – something that is impossible without expensive real-time sensors.

The objectives of this paper are to investigate the existence of some relations between the apparent features definable by machine vision for the moisture content of quince slices during dehydration, and to examine the use of artificial neural networks and regression based modelling to exploit all the extracted features in a single measurement tool.

MATERIAL AND METHODS

Sample preparation. We obtained the quince fruits (Cydonia Oblonga) used in this study from a local market. Fresh samples were selected manually and stored at a temperature of 20°C until the beginning of the experiment. For the drying experiment, discs of quince with a diameter of 20 mm and thickness of 7 mm were prepared. The samples were weighed before drying and the first-time images of the samples were captured with the resolution of 180 dpi and size of 1800 × 1600 pixels. The actual pixel size of the captured images was 7 pixel/mm. A CCD camera (Canon IXUS 960IS, 12.1 megapixel; Canon Inc., Tokyo, Japan) was used and mounted vertically at the distance of 30 cm over the samples. Quince slices were placed onr ceramic planes coated with heat-resistant black paint and dried in an oven dryer at three different temperatures (40, 50, and 60°C). For each temperature, 42 slices of the samples were used. A dry base of MC for the samples was calculated and used for equation developments in this project.

Image segmentation. The flowchart in Figure 1 shows the algorithm developed in this study to segment the images and extract the desired features. Image segmentation is the first step of image analysis. Optimal threshold value was applied to grey-scaled images to subtract the background from the images and obtain the binary image. After removing all undesirable objects from the background and filling the unwanted noisy holes (based on the 30 images investigated in this section, the area of noisy holes was 4.782 ± 0.102% of the region of interest in binary image) within the

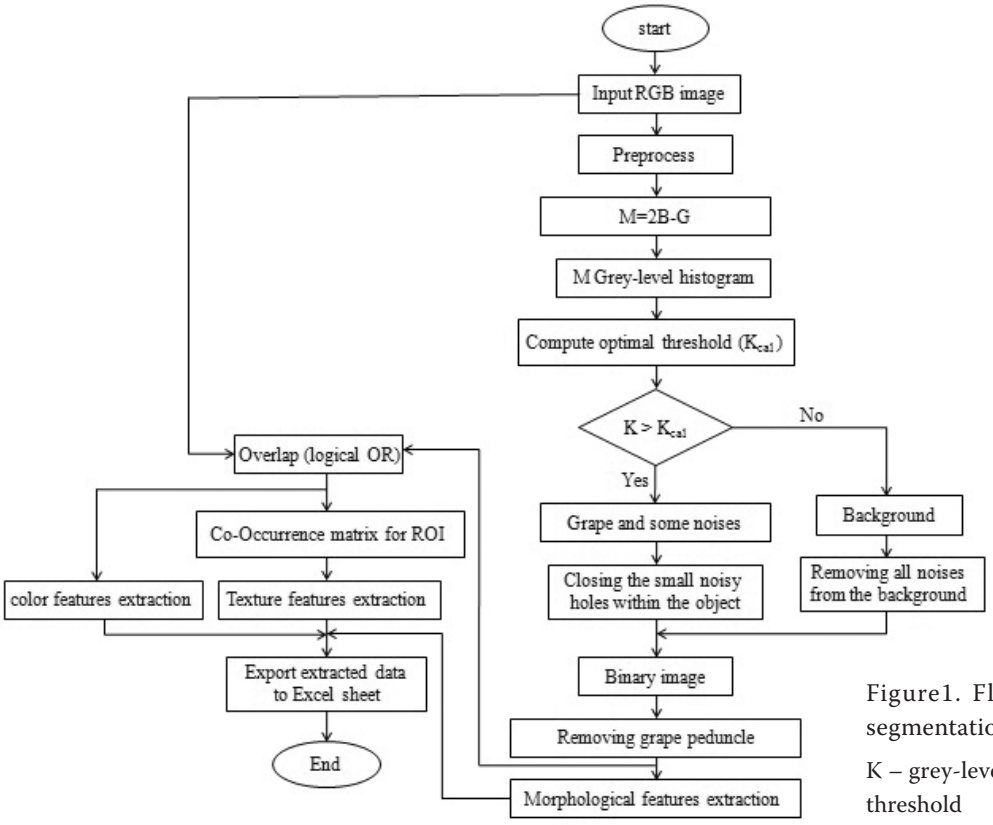

Figure1. Flowchart of the image segmentation and feature extraction

K – grey-level intensity; K_{cal} – optimal threshold

quince disc object, the final binary image was ready for extracting quantitative morphological data.

To remove the effects of the background pixel values from the colour and texture data, logical AND operator was applied to superimpose the original RGB images of the samples on the binary images gained from the last steps. The result was an image with omitted background. This image was then used to extract the colour and texture data.

Feature extraction. Six morphological features were calculated; area, perimeter, maximum, minimum and equivalent diameters, and surface roundness. The average values were determined of intensities for each colour component in RGB, HSI, and *L*a*b* colour spaces.

Grey-level co-occurrence matrix (GLCM) matrices were calculated for directions 0, 45, 90, and 135 degrees with a distance of one pixel between two adjacent pixels. The average of four developed matrices was determined to obtain the final co-occurrence matrix used for the texture feature extraction. Five textural features were determined for each grey-scale image.

Entropy: measures the disorder of an image. It achieves its largest value when all elements in GLCM matrix are equal (Gonzales & Woods 2002).

$$\text{Entropy} = \Sigma_i \Sigma_j C_{ij} \log C_{ij} \quad (1)$$

where: C_{ij} – (i,j) array of GLCM

Energy: also called Angular Second Moment (Haralick 1979) or Uniformity is the measure of textural uniformity of an image. Energy reaches its highest value when grey level distribution has either a constant or a periodic form (Gonzalez & Woods 2002).

$$\text{Energy} = \Sigma_i \Sigma_j C_{ij} \quad (2)$$

Inertia: also called contrast, is a measure of the amount of local variations present in an image. A high contrast value indicates a high degree of local variation (Park & Chen 2001).

$$\text{Inertia} = \Sigma_i \Sigma_j (i-j)^2 C_{ij} \quad (3)$$

Correlation: measures the correlation between the elements of the matrix. When correlation is high, the image will be more complex than when correlation is low.

$$\text{Correlation} = \Sigma_i \Sigma_j \frac{(i-\mu)(j-\mu_y) C_{ij}}{\sigma_i \sigma_j} \quad (4)$$

where: μ_x, μ_y – average and standard deviations of C_x, C_y

C_x, C_y are calculated as:

$$C_x(i) = \sum_{j-1}^{N_g} C_{ij} \text{ and } C_y(i) = \sum_{j-1}^{N_g} C_{ij} \quad (5)$$

where: N_g – number of grey levels

Inverse difference moment (IDM): measures image homogeneity. This parameter achieves its largest value when most of the occurrences in GLCM are concentrated near the main diagonal (Park & Chen 2001).

$$\text{IDM} = \Sigma_i \Sigma_j \frac{C_{ij}}{1 + (i-j)^2} \quad (6)$$

Analysis. All extracted features were exported to Excel sheets for later statistical analysis and plotting the figures. The data were analysed statistically using SPSS 17 software (SPSS Incorporation, Chicago, USA) to investigate if there was an acceptable relation between the MC of the samples and extracted features.

Several forms of relations between MC and extracted features were investigated to find the best equation for the moisture prediction including linear, logarithmic, inverse, and exponential relations between the MC and features. The best descriptive relations were selected based on the maximum determination coefficient (R^2) and the lowest Mean Square Error (MSE).

Neural Networks. Multilayer perceptron neural networks with back-propagation training algorithm were used to predict the MC of the samples. The values of colour, morphological and textural features were supplied as input neurons.

The input data were divided into three parts randomly, 60% for training, 20% for validation and 20% for network test (Nasirahmadi & Behroozi-Khazaei 2013). Several topologies of networks were developed and then compared. Subsequently, the network with the best performance was selected based on higher values of the R^2 and the lowest values of the root means square error (RMSE) (Menlik *et al*. 2010).

RESULTS AND DISCUSSION

Moisture content and time. The variations of the drying rate with the drying time for various temperatures of quince slices are shown in Figure 2. The values of MC changed rapidly in the first 5 h of drying. The initial MC was about 5.321 dry base – d.b. (= 5321% d.b. = 84.18% wet base – w.b.). Decimal dry basis MC values were used in this study for calculations. It is evident from Figure 2, that by increasing the drying temperature, the total drying time decreases,

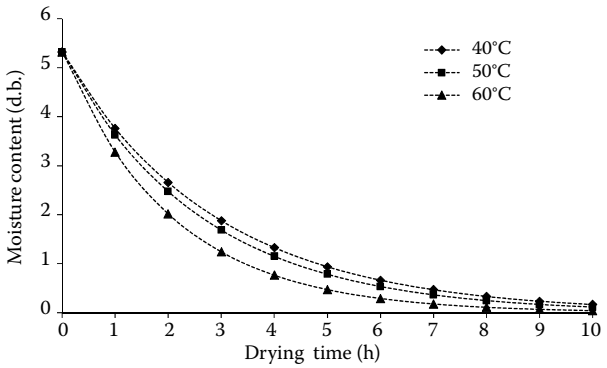

Figure 2. The variation of MC during the time for various drying temperatures

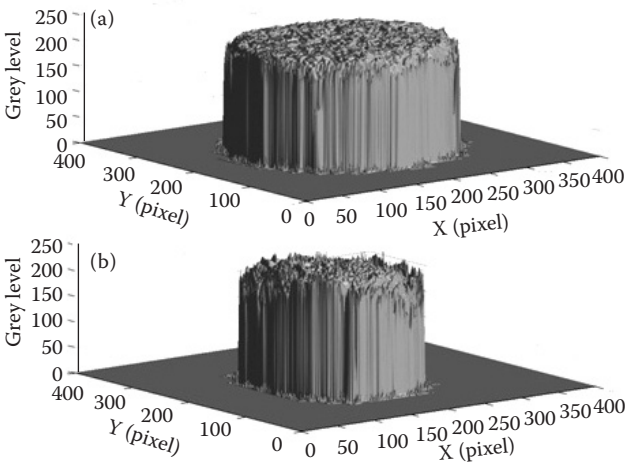

Figure 3. Grey-level intensities of quince disc images showing texture change: (a) before drying and (b) after 12 h drying

especially for higher MC values. Figure 3 indicates that the process of drying clearly affects the grey-level intensities of quince slice images which is a good numerical descriptor to track the changes in the apparent characteristics of food materials during processing or as a consequence of it (Chanona *et al*. 2003; Kerdpiboon & Devahastin 2007).

MC vs. morphological features. Figure 4 represents a gallery of images from a single quince disc at even hours during the drying process at the temperature of 50°C. The changes in the size and shape of the quince discs were evident as drying progressed. All morphological features decreased in the course of time passed. This result confirms previous reports regarding the morphological changes on grape tissue during drying (Ramos *et al*. 2004). It is also in agreement with the reports on apple slices (Fernández *et al*. 2005) and potato discs (Yadollahinia *et al*. 2009).

A linear relation with a good coefficient of correlation was achieved between the MC and each of the morphological features of the image separately, except for roundness (Table 1). High correlation coefficient values and the variance inflation factor within morphological features themselves showed that these features have multicollinearity. Therefore and because of the benefits of simpler relations and the importance of a higher process speed for real time projects, a simple relation was developed using the area and drying time to predict MC of quince slices (Table 2).

To derive a comprehensive equation, the time and temperature were also incorporated into MC prediction equations. Several forms of relations including linear, quadratic, exponential, and logarithmic were tested. The best results are presented in Table 3 while the Eq. (7) with the best R^2 (0.965) and the least MSE (0.361%) was selected.

Table 1. Correlation coefficients between morphological features and moisture content MC

Temperature (°C)	Area	Perimeter	Equivalent diameter	Minor diameter	Major diameter	Roundness
40	0.981	0.970	0.974	0.973	0.951	0.794
50	0.976	0.963	0.968	0.959	0.946	0.719
60	0.971	0.967	0.962	0.963	0.924	0.722

Table 2. Relations between moisture content (MC), time, and area of quince discs

	Temperature (°C)		
	40	50	60
$MC^{½} = c + ax + by$	$MC^{½} = -0.732 - 0.045$ time $+ 0.003$ area	$MC^{½} = -0.179 - 0.059$ time $+ 0.002$ area	$MC^{½} = -1.120 - 0.034$ time $+ 0.003$ area
t-value of (a)	−13.901 (0.000)	−20.834 (0.000)	−13.825 (0.000)
t-value of (b)	36.173 (0.000)	29.232 (0.000)	51.252 (0.000)
t-value of (c)	−10.174 (0.000)	−12.710 (0.000)	−21.661 (0.000)
R^2	0.973	0.974	0.963

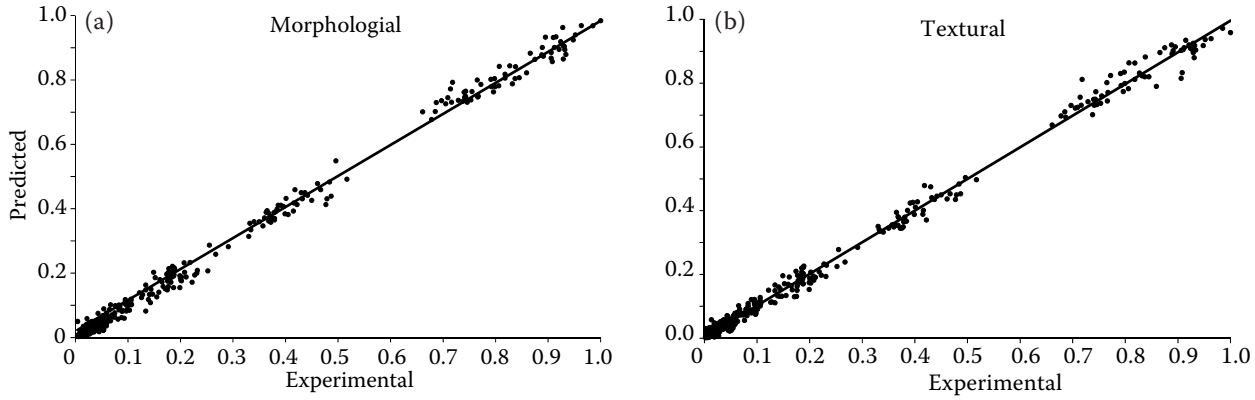

Figure 5. Normalised values of predicted and measured moisture content: (a) using area, time, and temperature and (b) using energy, time, and temperature

Table 3. Some of developed relations for moisture content (MC) prediction using time, temperature and area

Equation	R^2	MSE (%)
MC = –5.160 – 0.004 time + 0.005 temperature + 0.009 area	0.947	0.439
MC = (–0.616 – 0.004 time + 0.005 temperature + 0.003 area)^2	0.965	0.361
MC = (–36.009 + 0.387 time + 0.089 temperature + 0.051 area)$^{0.5}$	0.864	0.613
Ln (MC) = –0.428 – 0.193 time – 0.028 temperature + 0.003 area	0.954	0.401

MSE – mean square error

$$MC = (-0.616 - 0.040\ time - 0.004\ temperature + 0.003\ area)^2 \quad (7)$$

(67.72) (–8.46) (–23.53) (–12.23)
[0.000] [0.000] [0.000] [0.000]

The values in the parentheses and brackets are respectively *t*- and *P*-values for each coefficient. All of them are significant ($P < 1\%$). Equation (7) results in an acceptable prediction of MC of quince discs. The predicted versus measured values of MC are illustrated in Figure 5a. Prediction was more precise with lower MC values.

MC vs. colour features. There was no significant correlation between MC of quince slices and average as well as standard deviation values of the extracted colour components (Table 4). These results indicated that the colour features do not follow a distinct trend with the MC changes. Thus, the colour is not a suitable descriptor of MC value during drying in the case of quince drying.

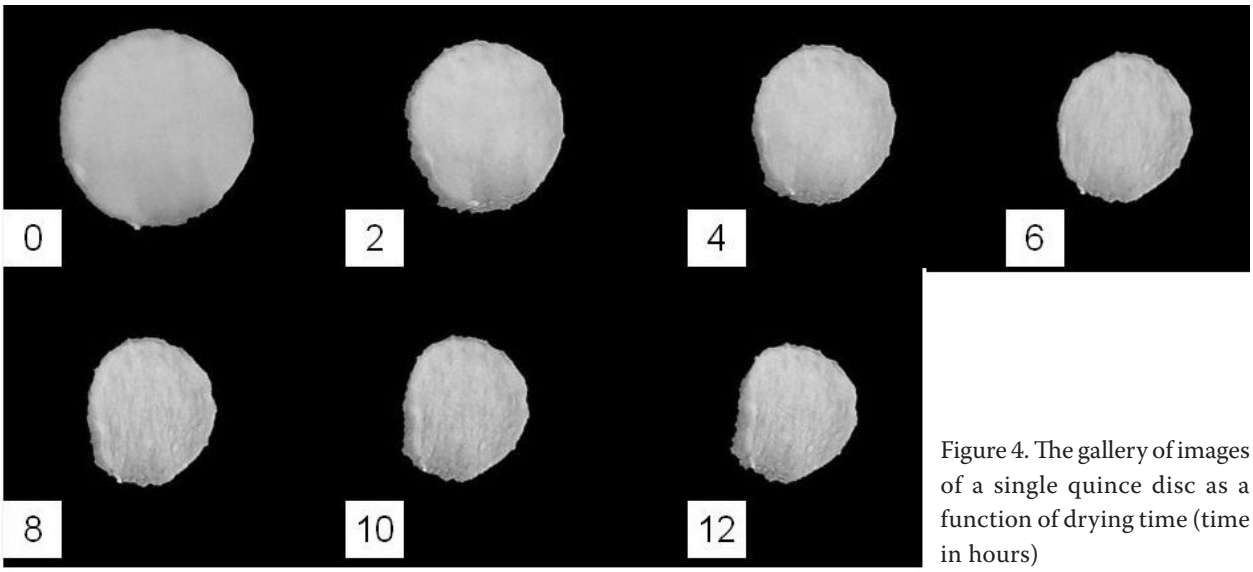

Figure 4. The gallery of images of a single quince disc as a function of drying time (time in hours)

Table 4. Correlation coefficients between colour features and moisture content

Temperature (°C)	R	G	B	H	S	V	L^*	a^*	b^*
40	–0.730	–0.185	–0.043	–0.200	–0.643	–0.732	–0.347	–0.544	–0.354
50	–0.643	–0.059	–0.299	0.128	–0.349	–0.645	–0.211	–0.570	0.185
60	–0.738	–0.104	0.170	–0.222	–0.698	–0.788	–0.272	–0.633	–0.549

R,G, B – Red, Green, Blue colour components in RGB colour space; H, S, and V – hue, saturation and intensity components in HSV colour space; L^*, a^*, b^* – lightness and chromatic components in $L^*a^*b^*$ colour space

Table 5. Correlation coefficients between texture features and moisture content

Temperature (°C)	Entropy	Energy	Inertia	Correlation	Inv. diff.
40	–0.715	0.964	–0.946	0.547	0.809
50	–0.737	0.947	–0.954	0.435	0.806
60	–0.716	0.942	–0.935	0.640	0.815

Table 6. Relations between moisture content (MC), time, and energy of quince discs

	Temperature (°C)		
	40	50	60
$MC^{½} = c + ax + by$	$MC^{½}$ = 0.215 – 0.029 time + 6.760 area	$MC^{½}$ = 0.644 – 0.052 time + 4.580 area	$MC^{½}$ = –0.151 – 0.001 time + 7.860 area
t-value of (a)	–6.082 (0.000)	–16.001 (0.000)	–0.192 (0.850)
t-value of (b)	27.290 (0.000)	27.443 (0.000)	40.010 (0.000)
t-value of (c)	3.523 (0.000)	15.834 (0.000)	–3.532 (0.000)
R^2	0.954	0.972	0.944

MC and textural features. High correlation coefficients were observed between MC and textural Energy as well as Inertia (Table 5). The R^2 of the regression relations decreased when the drying temperature increased. The same trend could be seen for the precision of equations developed to predict MC values. Several forms of equations were tested and finally the best equations were developed using, energy, drying time, and the square root of MC as follows (Table 6).

The *t*-value of the coefficient of drying time in the equation at 60°C was not significant and did not improve the precision of MC prediction equation.

Finally, several equations were evaluated to derive a comprehensive equation for predicting MC of quince slices using energy, drying time, and drying temperature. Table 7 shows some of the best relations while Eq. (8) (R^2 = 0.949 and MSE = 0.405%) was selected.

$$MC = (0.317 - 0.019\ time - 0.004\ temperature + 6.760\ area)^2 \quad (8)$$

(52.68) (–5.84) (–7.97) (–6.53)

[0.000] [0.000] [0.000] [0.000]

Regarding R^2, MSE, *t*- and *P*-values, Eq. (8) is a good predictor of MC based on textural data.

The scatter plot of the predicted MC using energy, time, and temperature vs. measured MC has been illustrated in Figure 5b. Similar to Figure 5a, the accuracy of prediction increases as MC decreases. It is possible to predict MC of the quince slices by considering textural features during drying. However, this is less efficient than the use of morphological features.

Results of neural networks. At last, all morphological, textural, and colour data were used in an ANN model. The results acquired from several topologies

Table 7. Some of developed relations for moisture content (MC) prediction using time, temperature and energy

Equation	R^2	MSE (%)
MC = –2.220 + 0.059 time + 0.007 temperature + 21.109 energy	0.917	0.497
$MC = (0.317 - 0.019\ time + 0.004\ temperature + 6.760\ energy)^2$	0.949	0.405
$MC = (-20.000 + 0.720\ time + 0.099\ temperature + 115.000\ energy)^{0.5}$	0.822	0.641
Ln (MC) = –0.428 – 0.169 time – 0.028 temperature + 7.909 energy	0.939	0.420

Table 8. Results of several MLP networks

ANN	Transfer function	Epoch	RMSE (%)	R^2
4-8-8-1	Tansig	16	0. 009	0.997
4-8-10-1	Tansig	16	0.011	0.996
4-10-10-1	Tansig	15	0.008	0.999
4-8-8-1	Logsig	15	0.011	0.996
4-8-10-1	Logsig	17	0.019	0.996
4-10-10-1	Logsig	14	0.017	0.996

ANN – Artificial Neural Network; Epoch – number of training cycles; RMSE – root means square error

of ANN are shown in Table 8. Regarding this table, the (4-10-10-1) MLP network with tangent sigmoid transfer function yielded the best results with a maximum R^2 value of 0.999, lowest values of the RMSE (0.008%). The plot of the predicted MC versus measured MC is shown in Figure 6. The developed ANN model can be used for the determination and prediction of drying behaviours of quince using image features.

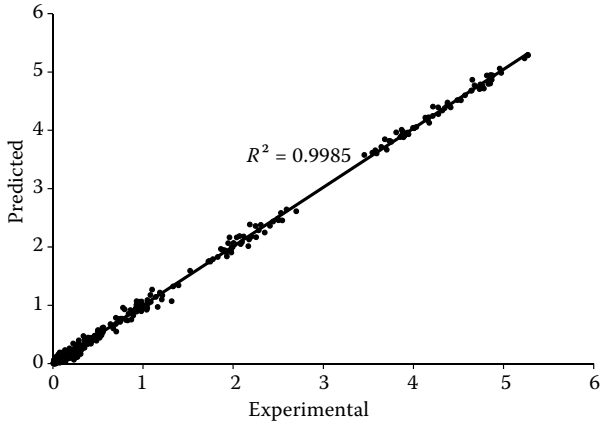

Figure 6. Performance of the ANN model for MC prediction

CONCLUSIONS

Quality control of products during a continuous drying process requires sensors that are capable of measuring the requested indices in a real-time mode. Direct measurement of MC through sampling of the product is undesirable because it interrupts the continuous flow of the materials. In this study, indirect measurement of MC was tried via measuring the visible characteristics of the samples. Such a kind of measurement is possible if there is a good agreement between the changes of visible features and the changes of MC. Therefore several experiments were conducted to investigate the correlation between the shape, texture and colour features of the samples and their corresponding MC.

Based on the results of the experiments which showed a good agreement between the texture and some shape features of the samples, it was concluded that the indirect measurement of the MC of quince slices is feasible especially when combinations of correlated features are used. The effective features were combined in a neural network model to determine the MC, whereas an R^2 up to 0.999 between the MC prediction and the measurement demonstrated its feasibility for the MC measurement of quince slices, on line.

References

Chanona P.J.J., Alamilla B.L., Farrera R.R.R., Quevedo R., Aguilera J.M., Gutiérrez L.G.F. (2003): Description of the convective air drying of a food model by means of the fractal theory. Food Science and Technology International, **9**: 207–213.

Cubillos F., Reyes A. (2003): Design of a model based on a modular neural network approach. Drying Technology, **21**: 1185–1195.

Du C.J., Sun D.W. (2004): Recent developments in the applications of image processing techniques for food quality evaluation. Trends in Food Science and Technology, **15**: 230–249.

Farkas I., Remenyi P., Biro B. (2000): A neural network topology for modeling grain drying. Computers and Electronics in Agriculture, **26**: 147–158.

Fernández L., Castillero C., Aguilera J.M. (2005): An application of image analysis to dehydration of apple discs. Journal of Food Engineering, **67**: 185–193.

Firatligil-Durmus E., Šárka E., Bubník Z. (2008): Image vision technology for the characterisation of shape and geometrical properties of two varieties of lentil grown in Turkey. Czech Journal of Food Sciences, **26**: 109–116.

Golpour I., Parian J.A., Chayjan R.A. (2013): Identification and classification of bulk paddy, brown and white rice cultivars with colour features extraction using image analysis and neural network. Czech Journal of Food Sciences, **32**: 280–287.

Gonzales R.C., Woods R.E. (2002): Digital Image Processing. 2nd Ed. Prentice-Hall, Inc., New Jersey.

Haralick R.M., Shanmugan K., Dinstein I. (1973): Textural Features for Image Classification. IEEE Transactions on Systems, Man, and Cybernetics, **3**: 610–621.

Jayas D.S., Paliwal J., Visen N.S. (2000): Multi-layer neural networks for image analysis of agricultural products. Journal of Agricultural Engineering Research, **77**: 119–128.

Kerdpiboon S. Devahastin S. (2007): Fractal characterization of some physical properties of a food product

under various drying conditions. Drying Technology, **25**: 135–146.

Kiranoudis C.T. Markatos N.C. (2000): Pareto design of conveyor-belt dryers. Journal of Food Engineering, **46**: 145–155.

Kit L., Spyridon Y., Papadakis E. (2004): A simple digital imaging method for measuring and analyzing color of food surfaces. Journal of Food Engineering, **61**: 137–142.

Menlik T., Özdemir M.B., Kirmaci V. (2010): Determination of freeze-drying behaviours of apples by artificial neural network. Expert Systems with Applications, **37**: 7669–7677.

Nasirahmadi A., Behroozi-Khazaei N. (2013): Identification of bean varieties according to color features using artificial neural network. Spanish Journal of Agricultural Research, **11**: 670–677.

Park B., Chen Y.R. (2001): Co-occurrence matrix texture features of multi-spectral images on poultry carcasses. Journal of Agricultural Engineering Research, **78**: 127–139.

Ramos I.N., Silva C.L.M., Sereno A.M., Aguilera J.M. (2004): Quantification of microstructural changes during first stage air drying of grape tissue. Journal of Food Engineering, **62**: 159–164.

Randulová Z., Tremlová B., Řezáčová-Lukášková Z., Pospiech M., Straka I. (2011): Determination of soya protein in model meat products using image analysis. Czech Journal of Food Sciences, **29**: 318–321.

Smékal O., Pipek P., Miyahara M., Jeleníková J. (2005): Use of video image analysis for the evaluation of beef carcasses. Czech Journal of Food Sciences, **23**: 240–245.

Wu D., Yang H., Chen X., He Y., Li X. (2008): Application of image texture for the sorting of tea categories using multi-spectral imaging technique and support vector machine. Journal of Food Engineering, **88**: 474–483.

Yadollahinia A., Jahangiri M. (2009): Shrinkage of potato slices during drying. Journal of Food Engineering, **94**: 52–58.

Received for publication September 27, 2013
Accepted after corrections March 7, 2014

Corresponding author:

Dr Adel Bakhshipour, Farm Machinery Department, Shiraz University, Shiraz, Iran;
E-mail: abakhshipour@shirazu.ac.ir